GEOLOGIJA *57/1*, 005-014, Ljubljana 2014

doi:10.5474/geologija.2014.001

# SEM/EDS characterisation of dusty deposits in precipitation and assessment of their origin

## SEM/EDS opredelitev prašnih usedlin v padavinah in ocena njihovega izvora

Miloš MILER

Geological Survey of Slovenia, Dimičeva ul. 14, SI–1000 Ljubljanat, Slovenia; e-mail: milos.miler@geo-zs.si

Prejeto / Received 23. 4. 2014; Sprejeto / Accepted 8. 5. 2014

*Key words*: dusty deposits, precipitation, source area, mineral composition, chemical composition, SEM/EDS, Slovenia
*Ključne besede*: prašne usedline, padavine, izvorno območje, mineralna sestava, kemična sestava, SEM/EDS, Slovenija

**Abstract**

Detailed scanning electron microscopy/energy dispersive spectroscopy (SEM/EDS) analysis of dusty material in rainfall residue, deposited and collected on February 19th 2014 in Ljubljana, was carried out with the intention to characterise it according to its chemical and mineral composition and to assess its origin. The material consists of poorly sorted and sharp-edged particles of mostly very fine-grained silt and clay fractions, which is consistent with long-range aerial transport. Particles are represented by illite, chlorite and kaolinite group clay minerals, quartz, feldspars, carbonates, accessory minerals and secondary Fe-oxy-hydroxide minerals. Quantities of minerals and illite/kaolinite ratio (4.5) correspond to dusts in rainfall residues originating from Moroccan Atlas, while chlorite/kaolinite ratio (2.8) agrees better with dust from central Libya. The element ratios Al/Si, Ca/Al, K/Ca, Mg/Al, Fe/Al and (Ca+Mg)/Fe in the studied dusty deposit are in good agreement with ratios in dusts from rainfall residues originating from Morocco and northern Mauritania. This was also confirmed by the trajectories of cloud movement that caused precipitation with dusty deposit, although the back trajectory HYSPLIT simulation of air masses indicated northern Mauritania, central Niger, southern Algeria, southwestern and central Libya as the most possible source regions.

**Izvleček**

Z vrstičnim elektronskim mikroskopom in energijsko disperzijskim spektrometrom (SEM/EDS) je bila opravljena raziskava prašnega ostanka v padavinah, ki se je odložil 19. februarja 2014 v Ljubljani. Cilj raziskave je bil opredeliti material glede na kemično in mineralno sestavo ter oceniti njegov izvor. Material sestavljajo slabo sortirani in ostrorobi delci, večinoma velikosti zelo drobnega melja in gline, kar nakazuje velike transportne razdalje. Delci so zastopani z glinenimi minerali illitove, kloritove in kaolinitove skupine, kremenom, glinenci, karbonati ter akcesornimi minerali in sekundarnimi železovimi minerali. Količine mineralov in razmerje illit/kaolinit (4,5) se ujemajo z usedlinami v dežju, ki izvirajo z maroškega Atlasa, medtem ko se razmerje klorit/kaolinit (2,8) dobro ujema s prahom iz osrednje Libije. Elementna razmerja Al/Si, Ca/Al, K/Ca, Mg/Al, Fe/Al in (Ca+Mg)/Fe v raziskani prašni usedlini se dobro ujemajo z razmerji v prahu v dežnih usedlinah, ki izvira iz Maroka in severne Mavretanije. To so potrdile tudi trajektorije gibanja oblakov, ki so prinesli padavine s prašnimi usedlinami. HYSPLIT simulacija povratnih trajektorij zračnih mas je nakazala, da so najverjetnejša izvorna območja severna Mavretanija, osrednji Niger, južna Alžirija, jugozahodna in osrednja Libija.

### Introduction

Solid airborne particles represent the highly variable component of the atmosphere. The quantity of airborne particles is controlled by numerous natural and anthropogenic factors, including natural weathering of bedrock and soil, anthropogenic activities, the distance from sources and meteorological conditions (Vanderstraeten et al., 2007). The retention time of solid airborne particles in the air depends to a great extent on their aerodynamic diameter, shape, structure and chemical characteristics (Girard, 2010; Neinavaie et al., 2000). Before deposition, particles are transported over various distances. Larger particles with a diameter greater than 10 µm are transported by air over short distances up to several kilometres, while smaller particles can travel several tens of kilometres (Guthmann, 1958; Neinavaie et al., 2000). In certain cases, strong winds blowing at high speeds across vast unvegetated surfaces can entrain and uplift small soil particles into the upper parts of the atmosphere, up to 12 kilometres high (troposphere and even stratosphere). These particles may then be transported over distances of several 100 or even several 1000 kilometres over other continents (Scheuvens et al., 2009) where they are eventually settled by dry or wet deposition (Schöner et al., 1993; Girard, 2010). Particles smaller than 10 µm, play an important

role in the formation of atmospheric precipitations. Under suitable atmospheric conditions, small solid particles act as condensation nuclei (Choël et al., 2006) around which water vapour condenses, resulting in the formation of cloud droplets or snowflakes. Large unvegetated areas, mostly extensive desert regions on Earth, represent the most important natural sources of dust in the atmosphere. The annual quantity of desert dust in the atmosphere transported over long distances is estimated at 0.5 to 5 billion tons (Perkins, 2001). Numerous studies of chemical and mineral composition of airborne desert dust transported over Europe and dust in the vicinity of larger deserts in Africa and Asia indicated 5 different dust source areas in North Africa (northern Algeria-Tunisia, southern Algeria-Mali, Atlas-Western Sahara-Morocco, Libya-Egypt, Chad-Sudan-Niger) and 6 areas in East Asia (Taklamakan, Gurbantunggut, Kumtaq-Qaidam, Northern Gobi, Southern Gobi, northeastern deserts (Otindag-Horquin-Hulun Buir)) (Scheuvens et al., 2009, Formenti et al., 2010). Among dust sources with smaller influence are also larger arid regions in Australia, South Africa, South America and the USA (Washington et al., 2003).

Occurrence of desert dust in precipitation is a common phenomenon in Europe and is also frequent in Slovenia. It has been recorded at least three times in Slovenia in the last three years (Trošt, 2011; Bolte & Koleša, 2013). On February 19th 2014 small amounts of dirty rainfall were occasionally reported from all over Slovenia, occurring from the early forenoon to the mid-afternoon, leaving behind yellow dusty deposits. According to data collected by the Environmental Agency of the Republic of Slovenia, the average daily concentrations of $PM_{10}$ and $PM_{2.5}$ in the air measured on that day at monitoring site in Ljubljana, located about 2 km east of sampling point, were 48 µm/m$^3$ and 53 µm/m$^3$, respectively, which were the highest values measured in February (Internet 1). The aim of this study was to characterise the dusty deposit in precipitation according to its chemical and mineral composition and to assess its origin.

## Materials and methods

A sample of dusty deposit was collected from a car windscreen after the rainfall on February 19th 2014 in the western part of Ljubljana. The quantity of the material was 0.096 g, which was below the quantity required for X-ray diffraction and chemical analysis, thus it was only analysed by the SEM/EDS. The particulate material was mounted on a double-sided carbon tape with a surface of 25 mm$^2$ and coated with a thin layer of carbon for conductivity and analysed with scanning electron microscopy coupled with energy dispersive spectrometry (SEM/EDS), which is commonly used in dust particle characterisation (Blanco et al., 2003; Formenti et al., 2010). The SEM/EDS analysis was carried out in a high vacuum using a JEOL JSM 6490LV SEM coupled with an Oxford INCA Energy 350 EDS system at 20 kV accelerating voltage, spot size 50 and 10 mm working distance. Mineral phases were assessed by calculating stoichiometric ratios from atomic % of constituent elements, acquired by the qualitative EDS X-ray point analysis with an acquisition time of 20-30 s, and comparison with atomic proportions of constituent elements in known stoichiometric minerals, obtained from mineral databases (Anthony et al., 2009; Barthelmy, 2010). The software was calibrated for quantification using pre-measured universal standards included in the EDS software, which is a basic standardisation procedure in fitted-standards EDS analysis (Goldstein et al., 2003), referenced to a Co optimisation standard. The correction of EDS data was performed on the basis of the standard ZAF-correction procedure included in the INCA Energy software (Oxford Instruments, 2006). The particle-size was determined by measuring their longest dimension using a measuring tool included in the JEOL SEM software (Jeol, 2007). Average mineral, as well as average elemental compositions of the sample were assessed from the distribution of constituent elements, obtained by the EDS elemental mapping of 6 fields-of-view at magnification of 1200× with an acquisition time of approximately 760 s, and by comparison with mineral grain percentage composition charts for sediments given by Compton (1962). All analyses were carried out at the Geological Survey of Slovenia. In order to define movement and sources of air masses that produced dusty deposit in precipitation, 62-hour back trajectories of air masses at various heights above the sampling point were simulated using a Hybrid-Single Particle Lagrangian Integrated Trajectory (HYSPLIT) modelling system (Draxler & Rolph, 2013), based on the Global Data Assimilation System (GDAS) database of the National Centres for Environmental Prediction (NCEP).

## Results and discussion

### Grain-size distribution

The grain-size distribution of dusty deposit material is shown in Fig. 1. The material is poorly to very poorly sorted and particles are mostly sharp-edged and irregularly shaped. Their roundness varies between angular to sub-rounded. The mean and median grain sizes of 364 measured particles are 4.8 ± 4.1 µm and 3.1 ± 4.4 µm, respectively, ranging from 0.5 µm to 28.8 µm. Most of the particles fall in the size range of 1 µm to 3 µm, representing very fine grained silt (21 %) and clay (22 %) fractions. About 26 % of all particles belong to clay fraction (< 2 µm). Grain sizes of about 88 % of particles are below 10 µm and thus belong to $PM_{10}$ fraction, of which 41 % are smaller than 2.5 µm and thus classified as $PM_{2.5}$ particles that affect human health causing respiratory problems and also greatly influence

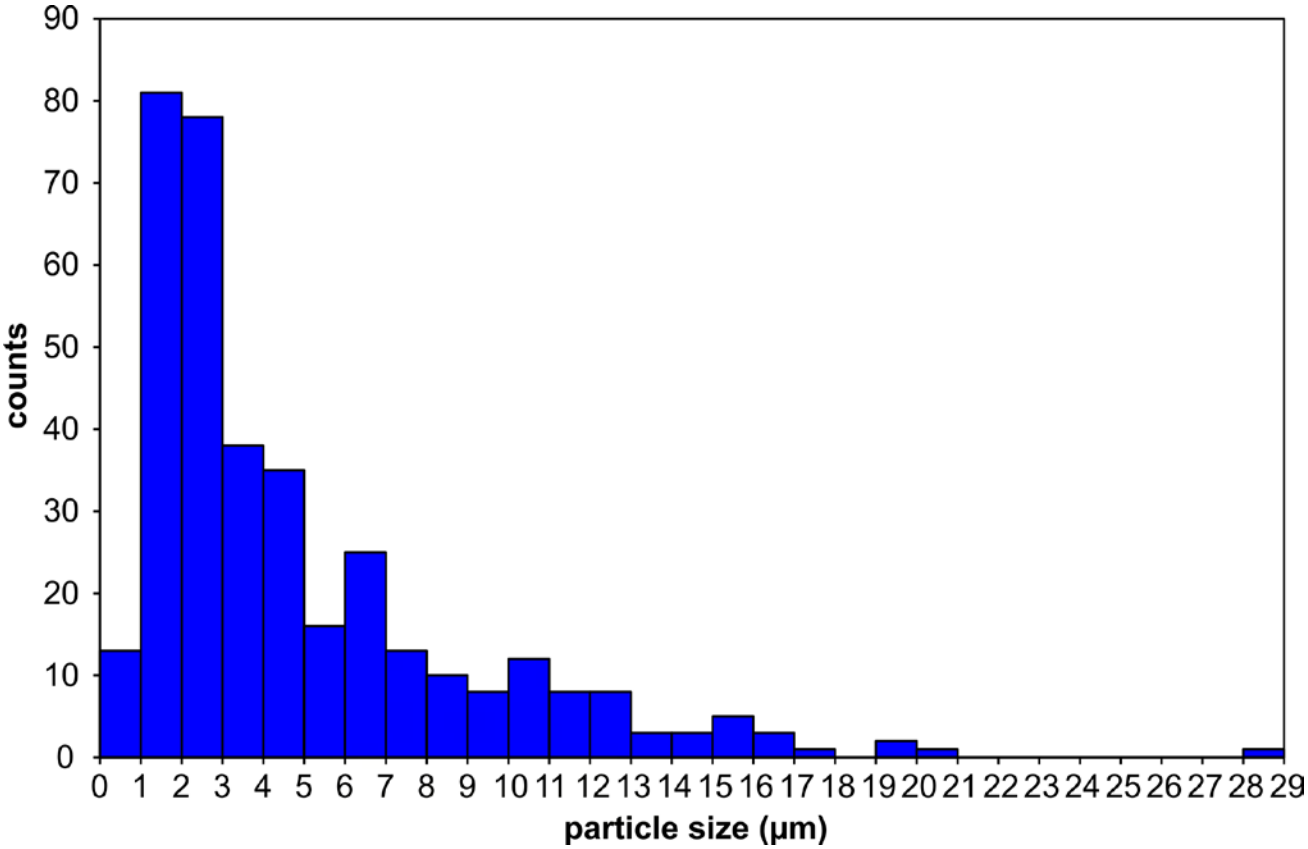


Fig. 1. Grain-size distribution of dusty deposit material.
Sl. 1. Porazdelitev velikosti delcev v prašni usedlini.

the global climate (Washington et al., 2003). The fine grained fractions are consistent with long-range aerial transport, although one would expect higher sorting degree. The grain size distribution and sorting depend on the strength of the winds during storms in the source areas. Generally, dusty deposits tend to get finer with increasing distance from their source regions, as coarse particles settle first, thus the mean grain sizes of the travelled dust range between 5 μm and 30 μm, which is the fine silt fraction (Goudie & Middleton, 2006). As reported by Rajot et al. (2008), the mean grain size of the dust after 1-2 day transport reaches 4.7 μm and remains constant afterwards. It can be thus assumed from the mean grain size (4.8 μm) of the studied dusty deposit that it travelled for nearly 2 days in the atmosphere before it was wet deposited. In addition, the grain size distribution of the dusty deposit analysed in this study agrees well with grain sizes of dust in rainfall residues collected in 2002 in SE Italy (Lecce), which was transported over a distance of about 2000 km from a source in the NW Sahara (Blanco et al., 2003).

## Mineral and chemical composition of individual particles

The SEM/EDS analysis showed that the sample of dusty deposit is composed mostly of clay minerals, quartz, feldspars and carbonates (Figs. 2a, b), which are all constituent minerals of soils. Accessory minerals and secondary weathering products of Fe-bearing accessory minerals are also present. Elemental composition of individual minerals is presented in Table 1.

Clay minerals are difficult to discern by means of SEM/EDS due to variable contents of volatile components (Blanco et al., 2003) and interchangeable cations and also presence of mixed layer clay variations. However, certain patterns in elemental composition were observed that enabled distinction between minerals. Thus, clay minerals belonging to illite, chlorite and kaolinite groups were recognised in analysed sample. Illite and chlorite both contain Mg, Fe, K, Ca, Al and Si. However, illite is characterised by higher contents of K and Al (Table 1), while chlorite has higher contents of Mg and Fe. According to composition of chlorite grains, chlorite group is represented mostly by chamosite and clinochlore. Kaolinite group minerals were determined on basis of Si/Al ratio, which is about 1. The $K_2O/(Al_2O_3+SiO_2)$ and $SiO_2/Al_2O_3$ ratios were also calculated for analysed illite and kaolinite group minerals and showed good correspondence with ratios in illite and kaolinite from literature data (Table 2). Illite and chlorite in the analysed sample occur as larger, irregularly shaped and elongated sub-angular grains as well as small elongated platelets, while kaolinite forms large massive sub-angular to sub-rounded grains and aggregates (Fig. 2a).

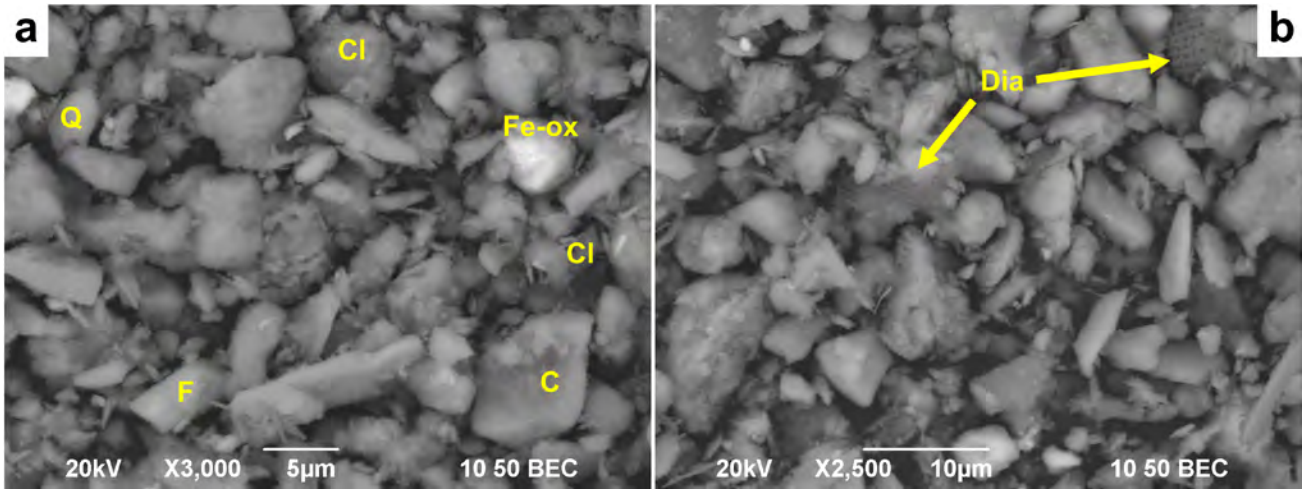


Fig. 2. SEM (BSE) images of the dusty deposit material. a) The material is composed of sharp edged quartz grains (Q), carbonates (C) and feldspars (F), while clay minerals (Cl) are rounded or form elongated platelets. b) Fragments of diatoms (Dia), which are morphologically similar to diatom frustules of the genus *Aulacoseira* spp. (Bristow et al., 2009), are also frequent.

Sl. 2. SEM (BSE) slike materiala prašne usedline. a) Material sestavljajo ostroroba zrna kremena (Q), karbonatov (C) in glinencev (F) ter zaobljena, podolgovata in lističasta zrna glinenih mineralov (Cl). b) Odlomki diatomej (Dia), ki so podobne frustulam diatomej rodu *Aulacoseira* spp. (Bristow et al., 2009), so tudi pogosti.

Other silicate minerals in dusty deposit are quartz and feldspars. Feldspars are mostly represented by orthoclase, which sometimes contains minor amounts of Na, and albite (Table 1). Quartz and feldspars occur as large irregularly shaped sub-angular grains and fragments or as angular euhedral crystals with pseudo-rhombohedral habit (Fig. 2a).

Carbonates are also abundant in deposited material and are generally represented with calcite and dolomite. They occur as smaller, mostly irregularly shaped sub-angular grains, however, subhedral and rhombohedral crystals were also found (Fig. 2a). Minor amounts of Si, Al and Fe (Table 1) measured in carbonates are due to presence of clay minerals around the carbonate grains and on their surfaces.

Accessory minerals and secondary weathering products of Fe-bearing accessory minerals are also present in dusty deposit, however they are rather scarce. Minor amounts of Mg, Al, Si, Ca and Fe (Table 1), which were detected in individual minerals, originate from the surrounding clay minerals. Accessory minerals are represented by phosphates apatite and monazite, Ti-rich oxides such as ilmenite and rutile, and silicates zircon and epidote. Apatite, which is mainly fluorapatite with minor amount of Cl, forms irregularly shaped sub-angular fragments and also prismatic hexagonal crystals. Monazite occurs as anhedral angular

Table 1. Element contents in individual minerals in dusty deposit (in at%) obtained by EDS analysis.
Tabela 1. Vsebnosti elementov v posameznih mineralih v prašni usedlini (v at%), določene z analizo EDS.

| Mineral | O | F | Na | Mg | Al | Si | P | Cl | K | Ca | Ti | Mn | Fe | Zr | La | Ce | Nd | Th |
|---|---|---|---|---|---|---|---|---|---|---|---|---|---|---|---|---|---|---|
| Illite | 75.9 | | | 1.2 | 8.1 | 11.9 | | | 2.3 | 0.2 | | | 0.3 | | | | | |
| Chlorite-chamosite | 71.8 | | | 2.2 | 7.6 | 13.6 | | | 0.9 | 0.4 | | | 3.7 | | | | | |
| Chlorite-clinochlore | 75.8 | | | 6.3 | 3.1 | 13.2 | | | 0.3 | 0.5 | | | 0.7 | | | | | |
| Kaolinite | 74.4 | | | | 11.5 | 13.2 | | | 0.2 | | | | 0.7 | | | | | |
| Calcite | 82.4 | | | | 0.4 | 1.0 | | | | 16.2 | | | | | | | | |
| Dolomite | 76.6 | | | 9.3 | 1.4 | 2.9 | | | | 9.5 | | | 0.3 | | | | | |
| Orthoclase | 69.2 | | | | 6.3 | 19 | | | 5.4 | | | | | | | | | |
| Albite | 67.4 | | 5.8 | | 6.6 | 20.3 | | | | | | | | | | | | |
| Epidote | 71 | | | | 8 | 11.9 | | | | 6.5 | | | 2.6 | | | | | |
| Zircon | 74 | | | 0.3 | 1.6 | 12.1 | | | | 0.5 | | | 0.4 | 11.2 | | | | |
| Apatite | 71.3 | 5.3 | | | 0.7 | 1.2 | 8 | 0.2 | | 13.2 | | | | | | | | |
| Monazite | 73.9 | | | 0.8 | 2.5 | 4.7 | 9.9 | | | 0.3 | | | 0.5 | | 2 | 3.9 | 1.3 | 0.2 |
| Ilmenite | 74.7 | | | 0.2 | 1.3 | 2.8 | | | | 0.1 | 11.1 | 3.1 | 6.6 | | | | | |
| Fe-oxy-hydroxide | 72.4 | | | 0.7 | 1.6 | 3.3 | | 0.4 | | 0.6 | | 0.2 | 20.8 | | | | | |

Table 2. $K_2O/(Al_2O_3+SiO_2)$ and $SiO_2/Al_2O_3$ ratios in illite and kaolinite from dusty deposit and literature data.

Tabela 2. Razmerja $K_2O/(Al_2O_3+SiO_2)$ in $SiO_2/Al_2O_3$ v illitu in kaolinitu iz prašne usedline in literaturnih podatkov.

| | Illite | Illite[a] | Kaolinite | Kaolinite[b] |
|---|---|---|---|---|
| $K_2O/(Al_2O_3+SiO_2)$ | 0.07 | 0.07 | 0.00 | 0.00 |
| $SiO_2/Al_2O_3$ | 1.67 | 1.94 | 1.31 | 1.11 |

[a]data from GAUDETTE et al., 1964
[b]data from ANTHONY et al., 2009

fragments, containing minor amounts of Th. Zircon occurs as relatively small anhedral angular fragments. Epidote is scarce and occurs as euhedral fragments of prismatic crystals. Ilmenite and rutile grains are mostly small anhedral and subhedral angular to sub-angular fragments surrounded by clay minerals. Secondary weathering products of accessory minerals are represented by Fe-oxy-hydroxides (Fig. 2a), which occur as sub-angular to sub-rounded grains and aggregates of minute crystals of Fe-oxy-hydroxides and clay minerals. Minor amounts of Mn and Cl were also detected in Fe-oxy-hydroxides, which could be incorporated into the structure of Fe-oxy-hydroxides (e.g. akaganéite) during their atmospheric transport over the sea due to presence of marine aerosols.

In addition to inorganic mineral grains, fragments of phytoplankton (Fig. 2b), such as diatoms, were also found in the sample, which could have a recent marine origin or could result from resuspension of detrital diatoms from areas of desiccated pluvial lakes in North Africa (FORMENTI et al., 2010). Morphologies and sizes of perforations in the skeletons of most of diatom fragments, observed in the sample, agree well with morphologies of diatom frustules of the genus *Aulacoseira* spp. found by BRISTOW et al. (2009) in diatomite and ECKARDT et al. (2005) in dust collected in the Bodele depression (Chad).

Average mineral composition, assessed from the distribution of constituent elements in the sample, showed that clay minerals are the most abundant in the studied dusty deposit, together representing approximately 49 % of all minerals. Illite occupies 26 % of the sample, chlorite represents 16 % and kaolinite only 6 %. Quartz occupies 22 % of the sample, while feldspars are represented by 8 %. Carbonates, dolomite and calcite, are also abundant, representing 17 % of all minerals in the sample. Accessory minerals and secondary Fe-oxy-hydroxide minerals are least abundant, together representing only 5 % of all minerals in the sample.

## Average elemental composition

Average elemental composition of the sample, obtained by the EDS elemental mapping, is given in Table 3. The sample is composed mainly of Si, Al, Fe, Ca, K and Mg, which can be ascribed to large amounts of clay minerals and carbonates. Minor and trace contents of S, Na, Cl and P

Table 3. Mean element contents with standard deviations (in wt%) in dusty deposit obtained by the EDS analysis.

Tabela 3. Povprečne vsebnosti elementov s standardnimi odkloni (v mas%) v prašni usedlini, določene z analizo EDS.

| Element | Mean content (n=4) | Standard deviation |
|---|---|---|
| O | 58.3 | 0.4 |
| Na | 0.5 | 0.2 |
| Mg | 1.4 | 0.1 |
| Al | 8.0 | 0.2 |
| Si | 22.0 | 0.7 |
| P | 0.1 | 0.0 |
| S | 0.2 | 0.0 |
| Cl | 0.1 | 0.0 |
| K | 1.6 | 0.2 |
| Ca | 2.4 | 0.2 |
| Ti | 0.4 | 0.0 |
| Fe | 4.5 | 0.3 |
| Cu | 0.3 | 0.1 |

and metals Ti and Cu were also detected in the sample. S, Na and Cl are either bound in the particle structure or adsorbed on the particle surfaces. Presence of these elements could indicate reactions between marine aerosols and dust particles (AVILA et al., 1997). Presence of P is most probably related to phosphate minerals apatite and monazite, while Ti is bound to ilmenite and rutile. The exact origin of Cu is not known. It could be anthropogenic or geogenic as it was found as a trace element in some Fe-oxy-hydroxides. Standard deviations of element contents are very low, indicating that the composition of the analysed sample is very homogeneous throughout the sample.

## Origin of dusty deposit material

Average elemental composition and mineral associations in dust material in the atmosphere are considered the most appropriate indicators of dust origin. Various clay mineral species, especially illite and kaolinite, are considered representative source tracers as their quantities and ratios are not considerably affected by physical and chemical fractionation processes at the soil-atmosphere interface and during long-range atmospheric transport (GLACCUM & PROSPERO, 1980; CAQUINEAU et al., 1998). The quantities of illite and carbonates in dust have been reported to increase from E to W and from S to N of Africa, while quantities of kaolinite generally decrease in these directions (e.g. SCHÜTZ & SEBERT, 1987; BLANCO et al., 2003; AVILA et al., 2007; SCHEUVENS et al., 2009; FORMENTI et al., 2010; SCHEUVENS et al., 2013). Thus highest illite/kaolinite ratios and carbonate contents (>10 %; FIOL et al., 2005) are expected for dusts originating

Table 4. Comparison between quantities of major minerals (in % of all identified minerals) in studied dusty deposit and dust in rainfall residues originating from different source regions in North Africa and relative errors (in %) to show closeness of agreement between compared quantities.

Tabela 4. Primerjava med količinami glavnih mineralov (v % vseh identificiranih mineralov) v raziskani prašni usedlini in prahu, ki izvira z različnih izvornih območij Severne Afrike ter relativne napake (v %) za prikaz ujemanja primerjanih količin.

| | This study | Moroccan Atlas (n=7)[e] | | Western Sahara (n=4)[e] | | Central Algeria (n=2)[e] | |
|---|---|---|---|---|---|---|---|
| Mineral | Quantity (%) | Quantity (%) | $E_{rel}$ (%) | Quantity (%) | $E_{rel}$ (%) | Quantity (%) | $E_{rel}$ (%) |
| Illite | 26.5 | 39.3 | 33 | 40.8 | 35 | 34.3 | 23 |
| Kaolinite | 5.9 | 3.6 | 65 | 7.6 | 23 | 12.5 | 53 |
| Quartz | 22.3 | 20.6 | 8 | 17.5 | 27 | 14.5 | 54 |
| Feldspar | 7.6 | 3.6 | 108 | 3.4 | 124 | 2.5 | 203 |
| Carbonate | 16.8 | 17.1 | 2 | 12.0 | 40 | 1.9 | 784 |
| Average $E_{rel}$ | | | 43 | | 50 | | 223 |

[e]data from AVILA et al., 1997

from Northwest Africa. The quantities of major minerals (clay minerals, quartz, feldspars and carbonates) in the studied dusty deposit were compared with mean quantities in samples of red dust deposited in rainwater from northeastern Spain (AVILA et al., 1997), originating from three different source regions: Moroccan Atlas, Western Sahara and central Algeria (Table 4). In order to assess the most possible source of the studied dusty deposit, the closeness of agreement between mineral quantities in studied dusty deposit and mean quantities in red dust samples from different sources was defined by means of calculating relative error $E_{rel} = (X_{sd} - X_{rd}/X_{rd}) \cdot 100\%$, where $X_{sd}$ is quantity of mineral in studied dusty deposit and $X_{rd}$ is quantity of mineral in red dust deposit. Relative error, calculated for illite (23 %), showed best fit with red dust originating from central Algeria, relative error for kaolinite (23 %) showed best agreement with red dust from Western Sahara, while lowest relative errors for quartz (8 %), feldspars (108 %) and carbonates (2 %) were calculated for dust originating from Moroccan Atlas. However, the average relative errors calculated for all minerals in each source group were 43 %, 50 % and 223 % for red dusts from Moroccan Atlas, Western Sahara and central Algeria, respectively (Table 4). Thus, the lowest average relative error was obtained for red dust from Moroccan Atlas and it can be presumed that Moroccan Atlas was also the most probable source of the studied dusty deposit. The illite/kaolinite (I/K) and chlorite/kaolinite (C/K) ratios calculated for the studied dusty deposit are relatively high and amount to 4.3 and 2.7, respectively. This is in agreement with high I/K ratios in dust originating from Moroccan Atlas (>4; AVILA et al., 1997; SCHEUVENS et al., 2013), while C/K ratio is much higher than that reported for samples from Atlas and northern Algeria regions and western coast of North Africa (>1) (CHESTER et al., 1971; PROSPERO, 1981; AVILA et al., 1997; SCHEUVENS et al., 2013). The C/K ratio thus corresponds better to ratios in dusts from central Libya (<2.6) (O'HARA et al., 2006). However, it has also been reported that C/K ratios from dust samples from northern source areas vary considerably (SCHEUVENS et al., 2013). Thus higher C/K ratios may also be possible in dusts from Northwest Africa. Deviations and wide ranges of mineral quantities and ratios between clay mineral species exist possibly due to heterogeneous geological composition, differential weathering and soil erosion, mixing of dust material transported by winds blowing from neighbouring source areas and wind conditions (e.g. SCHEUVENS et al., 2013).

The clay mineralogy of soils generally differs from source to source and so does the average elemental composition. Element ratios Al/Si, Ca/Al, K/Ca, Mg/Al, Fe/Al and (Ca+Mg)/Fe vary between source regions and can thus be used as indicators of dust source areas (BLANCO et al., 2003; AVILA et al., 2007; FORMENTI et al., 2010; MARCONI et al., 2014). Element ratios Al/Si, Ca/Al, K/Ca, Mg/Al, Fe/Al and (Ca+Mg)/Fe calculated for the studied dusty deposit and their comparison with ratios in dusts from rainfall residues sourced from North Africa are presented in Table 5.

Table 5. Element ratios in the studied dusty deposit compared with dust originating from North Africa and relative errors (in %) to show closeness of agreement between compared values.

Tabela 5. Razmerja elementov v raziskani prašni usedlini v primerjavi s prahom iz Severne Afrike in relativne napake (v %) za prikaz ujemanja primerjanih vrednosti.

| Element ratio | This study | North Africa | $E_{rel}$ (%) |
|---|---|---|---|
| Al/Si | 0.36 | 0.41[c] | 11 |
| Ca/Al | 0.30 | 0.37[c] | 18 |
| K/Ca | 0.64 | 0.73[c] | 12 |
| Mg/Al | 0.18 | 0.18[d] | 0 |
| Fe/Al | 0.56 | 0.59[d] | 5 |
| (Ca+Mg)/Fe | 0.86 | 0.62[d] | 39 |

[c]data from BLANCO et al., 2003
[d]data from AVILA et al., 2007

Table 6. Comparison between element ratios in studied dusty deposit and dust in rainfall residues originating from different source regions in North Africa and relative errors (in %) to show closeness of agreement between compared values.

Tabela 6. Primerjava med razmerji elementov v raziskani prašni usedlini in prahu, ki izvira z različnih izvornih območij Severne Afrike ter relativne napake (v %) za prikaz ujemanja primerjanih vrednosti.

| | This study | Libya & S. Mauritania[c] | | S. Algeria & Niger[c] | | S. Algeria & N. Libya[c] | | Morocco & N. Mauritania[c] | |
|---|---|---|---|---|---|---|---|---|---|
| | Element ratio | Element ratio | $E_{rel}$ (%) | Element ratio | $E_{rel}$ (%) | Element ratio | $E_{rel}$ (%) | Element ratio | $E_{rel}$ (%) |
| Al/Si | 0.36 | 0.5 | 27 | 0.48 | 24 | 0.45 | 19 | 0.41 | 11 |
| Ca/Al | 0.30 | 0.2 | 51 | 0.23 | 32 | 0.27 | 12 | 0.37 | 18 |
| K/Ca | 0.64 | 1.5 | 57 | 1.27 | 50 | 1.25 | 49 | 0.73 | 12 |
| Average $E_{rel}$ | | | 45 | | 35 | | 27 | | 14 |

[c]data from BLANCO et al., 2003

Most of element ratios in studied dusty deposit are somewhat lower compared to those reported in dusts from North Africa (BLANCO et al., 2003; AVILA et al., 2007) probably due to higher amounts of feldspars, kaolinite, quartz and carbonates. However, calculated relative errors showed relatively good agreement. The (Ca+Mg)/Fe ratio is a bit higher than in dusts from North Africa, which is related with higher carbonate content in the studied sample. This implies that carbonates in the studied sample were not significantly affected by dissolution processes during atmospheric transport, which usually decreases element ratios (AVILA et al., 2007), including the (Ca+Mg)/Fe ratio. A comparison with element ratios Ca/Al, K/Ca and Al/Si in dusts from rainfall residues, collected in SE Italy (Lecce) and originating from four different source areas: Libya and southern Mauritania, southern Algeria and Niger, southern Algeria and northern Libya, and Morocco and northern Mauritania (BLANCO et al., 2003) was also made in order to assess which dust source region is the most possible source of the studied dusty deposit (Table 6). With the exception of Ca/Al ratio, which agrees best with ratio in dust originating from southern Algeria and northern Libya (12 % relative error), all other element ratios in studied dusty deposit indicate the origin from Morocco and northern Mauritania. The average relative errors calculated for all element ratios in each source group were 45 %, 35 %, 27 % and 14 % for dust residues sourced from Libya and southern Mauritania, southern Algeria and Niger, southern Algeria and northern Libya, and Morocco and northern Mauritania, respectively (Table 6). The highest degree of concordance is observed between the studied dusty deposit and dust residues originating from Morocco and northern Mauritania.

The 62-hour cloud movement trajectories, which were constructed on the basis of hourly satellite cloud images from 16th February at 23:00 UTC to 19th February 2014 at 13:00 UTC (INTERNET 2), showed that the clouds that caused precipitation with dusty deposit originated from three different regions (Fig. 3). Clouds that caused precipitation in the early forenoon (yellow trajectory) formed over northern Mauritania (the whole trajectory could not be shown) and moved towards northeast over northern Mali, across Algeria, Mediterranean, Sardinia and Italy towards Slovenia. The grey and red trajectories indicate movement of clouds that brought precipitation in the mid-afternoon. The grey trajectory shows clouds that formed over northwestern part of Algeria, moved slowly across Moroccan Atlas all the way to southern Spain then back to northeastern Morocco and northern Algeria, across the Mediterranean where they gained on velocity, over Sardinia and northern Italy to Slovenia. It can be seen from the trajectories in Fig. 3 that the residence time of clouds was about 30 hours (48 % of the trajectory time) over Morocco, 14 hours (23 % of the trajectory time) over Algeria, 12 hours (19 % of the trajectory time) over Mediterranean and 6 hours (10 % of the trajectory time) over Sardinia, Italy and Adriatic Sea before they reached Slovenia. As clouds spent nearly half of the trajectory time over Morocco, this area can be considered as the most possible source region, which is also consistent with the source areas assessed from mineral and chemical composition of the studied dusty deposit. The red trajectory shows clouds that formed over the Atlantic Ocean and moved towards south across Morocco, northern Algeria, Mediterranean, Corsica, Italy and Adriatic to Slovenia. The residence times of these clouds were about 38 % of the trajectory time over the Atlantic, 16 % over Morocco, 23 % over Algeria, 11 % over Mediterranean and 11 % over Corsica, Italy and Adriatic Sea before reaching Slovenia. The 62-hour back trajectory HYSPLIT simulation showed that air masses, which were located at 2500, 3000, 3500, 4000, 4500, 7500 and 8000 m a.g.l. above the sampling site at the time of deposition (19th February 2014 at 13:00 UTC), originated from low altitudes in northern Mauritania, central Niger, southern Algeria, southwestern and central Libya and thus could have risen and transported the dusty material (Fig. 4). Four of the back trajectories ended over Libya, two over northern Mauritania and one over Niger and Algeria, thus the most significant source appears to be Libya. The air masses

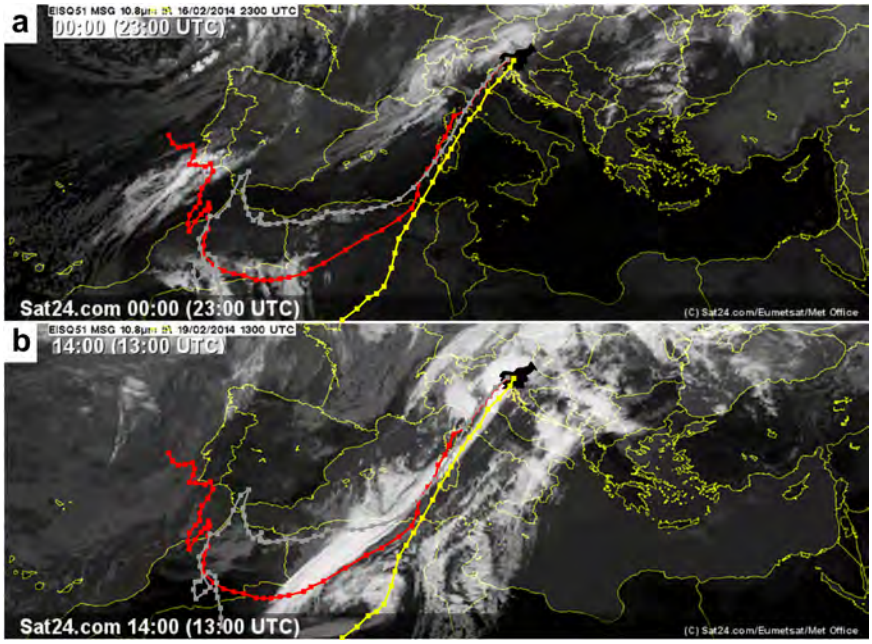


Fig. 3. Satellite cloud images and 62-hour cloud movement trajectories, constructed on the basis of hourly satellite cloud images from a) 16th February at 23:00 UTC to b) 19th February 2014 at 13:00 UTC (Internet 2).

Sl. 3. Satelitski sliki oblakov in 62 urne trajektorije gibanja oblakov, izdelane na osnovi urnih satelitskih slik oblakov od a) 16. februarja ob 23:00 UTC do b) 19. februarja 2014 ob 13:00 UTC (Internet 2).

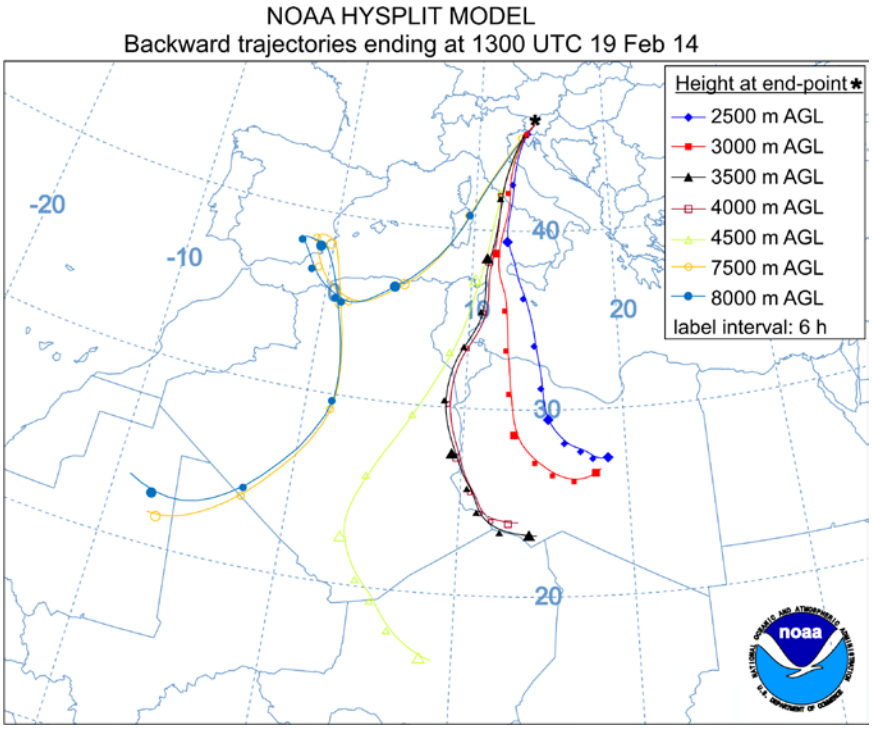


Fig. 4. Display of 62-hour air mass back trajectories, which were located at 2500, 3000, 3500, 4000, 4500, 7500 and 8000 m a.g.l. above the sampling site at the time of deposition (19th February 2014 at 13:00 UTC), constructed using HYSPLIT simulation (Internet 1).

Sl. 4. Prikaz 62 urnih povratnih trajektorij zračnih mas, ki so bile v času padavin (19. februar ob 13:00 UTC) locirane 2500, 3000, 3500, 4000, 4500, 7500 in 8000 m nad tlemi, izdelanih s HYSPLIT simulacijo (Internet 1).

originating from northern Mauritania moved relatively fast, spending only 3 % of the trajectory time over the source area. The residence times of air masses from Libya over their source areas were about 56 % of the trajectory time, while the air masses originating from Niger and Algeria travelled over the source areas for about 77 % of their trajectory time. These findings are not in agreement with the results of elemental and mineralogical analyses. However, according to Marconi et al. (2014), it is often difficult to assess all important source areas from back trajectory simulation data due to uncertainties in associating air mass trajectories with their source areas, especially when air masses are travelling within boundary layers.

## Conclusions

Dusty material in rainfall residue, deposited and collected on February 19th 2014 in Ljubljana, was analysed using SEM/EDS and characterised according to grain size, morphology, elemental and mineral composition. The analysis showed that the dusty material consists of poorly sorted and sharp-edged particles of mostly very fine-grained silt and clay fractions (size range 1-3 µm), which is consistent with long-range aerial transport. Particles are mostly represented by clay minerals of illite (26 %), chlorite (16 %) and kaolinite (6 %) groups. Other silicates are quartz (22 %) and feldspars (8 %), mostly orthoclase and albite. Carbonates, mostly dolomite and calcite,

represent 17 % of all minerals. While accessory minerals, such as fluorapatite, monazite, ilmenite, rutile, zircon and epidote, and secondary Fe-oxy-hydroxide minerals, represent 5 % of all minerals in the sample. Fragments of phytoplankton, such as diatom frustules, are also present. Quantities of clay minerals, quartz, feldspars and carbonates and also illite/kaolinite ratio (4.3) corresponded with dusts in rainfall residues originating from Moroccan Atlas, while chlorite/kaolinite ratio (2.7) agreed better to dusts from central Libya. The comparison between element ratios Al/Si, Ca/Al, K/Ca, Mg/Al, Fe/Al and (Ca+Mg)/Fe in the studied dusty deposit and ratios in dusts from North Africa showed that element ratios, with the exception of (Ca+Mg)/Fe in studied deposit were somewhat lower, but still in relatively good agreement, especially with ratios in dusts from rainfall residues originating from Morocco and northern Mauritania. The cloud movement trajectories showed that the clouds that caused precipitation with dusty deposit originated from northern Mauritania, northwestern part of Algeria and the Atlantic Ocean. The clouds then moved across northern Mali, northwestern part of Algeria and northern Morocco. The results of back trajectory HYSPLIT simulation of air masses indicated northern Mauritania, central Niger, southern Algeria, southwestern and central Libya as the most possible source regions. However, these were not in agreement with the results of elemental and mineralogical analyses and the differences were ascribed to uncertainties in associating air mass trajectories with their source areas. Thus, considering all dust origin indicators, mineralogical and chemical, the studied dusty deposit most probably originates from the areas of Moroccan Atlas and northern Mauritania.

**Acknowledgements**

The author acknowledges financial support from the state budget by the Slovenian Research Agency obtained through the research program "Mineral resources" (No. P1-0025).

## References

Anthony, J. W., Bideaux, R. A., Bladh, K. W. & Nichols, M. C. 2009: The Handbook of Mineralogy [online]. Mineralogical Society of America, [cited 11.8.2011]. Available from world wide web: < http://www.handbookofmineralogy.org/>.

Avila, A., Queralt-Mitjans, I. & Alarcón, M. 1997: Mineralogical composition of African dust delivered by red rains over northeastern Spain. J. Geophys. Res., 102/D18: 21977–21996.

Avila, A., Alarcón, M., Castillo, S., Escudero, M., García Orellana, J., Masqué, P. & Querol, X. 2007: Variation of soluble and insoluble calcium in red rains related to dust sources and transport patterns from North Africa to northeastern Spain. J. Geophys. Res., 112/D5: D05210, doi:10.1029/2006JD007153.

Barthelmy, D. 2010: The Mineralogy Database [online]. [cited 11.8.2011]. Available from world wide web: < http://webmineral.com/>.

Blanco, A., Dee Tomasi, F., Filippo, E., Manno, D., Perrone, M. R., Serra, A., Tafuro, A. M. & Tepore, A. 2003: Characterization of African dust over southern Italy. Atmos. Chem. Phys., 3: 2147-2159, doi:10.5194/acp-3-2147-2003.

Bolte, T. & Koleša, T. 2013: Influence of the Saharan sand on the concentration of PM10 particles in the year 2012: Report (in Slovene). Environmental Agency of the Republic of Slovenia, Ljubljana: 13 p.

Bristow, C. S., Drake, N. & Armitage, S. 2009: Deflation in the dustiest place on Earth: The Bodélé Depression, Chad. Geomorphology, 105/1–2: 50-58, doi: 10.1016/j.geomorph.2007.12.014.

Caquineau, S., Gaudichet, A., Gomes, L., Magonthier, M. C. & Chatenet, B. 1998: Saharan dust: clay ratio as a relevant tracer to assess the origin of soil-derived aerosols. Geophys. Res. Lett., 25: 983-986, doi:10.1029/98gl00569.

Chester, R., Elderfield, H. & Griffin, J. J. 1971: Dust transported in the north-east and south-east trade winds in the Atlantic Ocean. Nature, 233: 471–474.

Choël, M., Deboudt, K., Flament, P., Lecornet, G., Perdrix, E. & Sobanska, S. 2006: Fast evolution of tropospheric Pb- and Zn-rich particles in the vicinity of a lead smelter. Atmos. Environ., 40: 4439–4449.

Compton, R. R. 1962: Manual of field geology, 4th edition. John Wiley & sons, New York: 378 p.

Draxler, R. R. & Rolph, G. D. 2013: HYSPLIT (HYbrid Single-Particle Lagrangian Integrated Trajectory). Model access via NOAA ARL READY Website <http://www.arl.noaa.gov/HYSPLIT.php>. NOAA Air Resources Laboratory, College Park, MD.

Eckardt, F. D., Coetzee, S. H. & Washington, R. 2005: SEM view of world's most significant dust cloud sampled at Chicha, The Chad, Bodele Depression, Sahara. Microscopy Society of Southern Africa Conference Proceedings, 35: 23.

Fiol, Ll. A., Fornós, J. J., Gelabert, B. & Guijarro, J. A. 2005: Dust rains in Mallorca (Western Mediterranean): their occurrence and role in some recent geological processes. Catena, 63: 64-84.

Formenti, P., Schuetz, L., Balkanski, Y., Desboeufs, K., Ebert, M., Kandler, K., Petzold, A., Scheuvens, D., Weinbruch, S. & Zhang, D. 2010: Recent progress in understanding physical and chemical properties of mineral dust. Atmos. Chem. Phys. Discuss., 10: 31187–31251, doi:10.5194/acpd-10-31187-2010.

Gaudette, H. E., Eades, J. L. & Grim, R. E. 1964: The Nature of Illite. Clay. Clay Miner., 13/1: 33–48.

Girard, J. E. 2010: Principles of environmental chemistry, 2nd edition. Jones & Bartlett Publishers, Sudbury: 687 p.

Glaccum, R. A. & Prospero, J. M. 1980: Saharan aerosols over the tropical north Atlantic-mineralogy. Mar. Geol., 37: 295–321.

Goldstein, J., Newbury, D., Joy, D., Lyman, C., Echlin, P., Lifshin, E., Sawyer, L. & Michael, J. R. 2003: Scanning electron microscopy and x-ray microanalysis, 3rd edition. Kluwer Academic/ Plenum Publishers, New York: 689 p.

Goudie, A. S. & Middleton, N. J. 2006: Desert Dust in the Global System. Springer: Berlin and New York: 298 p.

Guthmann, K. 1958: Das Problem „Reinhaltung der Luft“ unter besonderer Berücksichtigung der Eisenhütten-,insbesondereStahlwerksbetriebe. Radex-Rundschau, 1: 3–30.

Jeol 2007: JSM-6490LV scanning electron microscope, instruction manual. JEOL Ltd., Tokyo: 187 p.

Marconi, M., Sferlazzo, D. M., Becagli, S., Bommarito, C., Calzolai, G., Chiari, M., di Sarra, A., Ghedini, C., Gómez-Amo, J. L., Lucarelli, F., Meloni, D., Monteleone, F., Nava, S., Pace, G., Piacentino, S., Rugi, F., Severi, M., Traversi, R. & Udisti, R. 2014: Saharan dust aerosol over the central Mediterranean Sea: $PM_{10}$ chemical composition and concentration versus optical columnar measurements. Atmos. Chem. Phys., 14: 2039-2054, doi:10.5194/acp-14-2039-2014.

Neinavaie, H., Pirkl, H. & Trimbacher, C. 2000: Herkunft und Charakteristik von Stäuben: Research report. Umweltbundesamt, Vienna: 61 p.

O'Hara, S. L., Clarke, M. L. & Elatrash, M. S. 2006: Field measurements of desert dust deposition in Libya. Atmos. Environ., 40: 3881–3897.

Oxford Instruments 2006b: INCA Energy Operator Manual. Oxford Instruments Analytical Ltd., High Wycombe: 84 p.

Perkins, S. 2001: Dust, the thermostat. Sci. News, 160: 200–201.

Prospero, J. M. 1981: Arid regions as sources of mineral aerosols in the marine atmosphere. Geol. S. Am. S., 186: 71–85.

Rajot, J. L., Formenti, P., Alfaro, S., Desboeufs, K., Chevaillier, S., Chatenet, B., Gaudichet, A., Journet, E., Marticorena, B., Triquet, S., Maman, A., Mouget, N. & Zakou, A. 2008: AMMA 20 dust experiment: an overview of measurements performed during the dry season special observation period (SOP0) at the Banizoumbou (Niger) supersite. J. Geophys. Res., 113: D00C14, doi:10.1029/2008jd009906.

Scheuvens, D., Schütz, L., Kandler, K., Ebert, M. & Weinbruch, S. 2009: Composition of Saharan dust and its possible source regions-a review. European Aerosol Conference 2009. Abstract T052A17.

Scheuvens, D., Schütz, L., Kandler, K, Ebert, M. & Weinbruch, S. 2013: Bulk composition of northern African dust and its source sediments-A compilation. Earth-Sci. Rev., 116: 170–194.

Schöner, W., Staudinger, M., Winiwarter, W. & Pichlmayer, F. 1993: Dating of snow samples from snow pits at Sonnblick, Austrian Alps as a tool for interpretation of chemical analysis. In: Borell, P. M. et al. (eds.): The Proceedings of EUROTRAC Symposium '92. SPB Academic Publishing, The Hague: 753–756.

Schütz, L. & Sebert, M. 1987: Mineral aerosols and source identification. J. Aerosol Sci., 18: 1–10.

Trošt, M. 2011: Detection of Saharan dust in troposphere (in Slovene): Diploma thesis. University of Ljubljana, Faculty of mathematics and physics. Ljubljana: 58 p.

Vanderstraeten, P., Lénelle, Y., Meurrens, A., Carati, D., Brenig, L. & Offer, Z. Y. 2007: Temporal variations of airborne particles concentration in the Brussels environment, Environ. Monit. Assess., 132: 253–262.

Washington, R., Todd, M., Middleton, N. J. & Goudie, A. S. 2003: Dust-Storm source areas determined by the Total Ozone Monitoring Spectrometer and surface observations. Ann. Assoc. Am. Geogr., 93: 297–313.

Internet 1: http://www.arso.gov.si/zrak/kakovost%20zraka/podatki/ (4.4.2014)

Internet 2: http://www.sat24.com/history.aspx (17.3.2014)